Simultaneous determination of the index and absorption gratings in multiple quantum well photorefractive devices designed for laser ultrasonic sensor

T. Shimura, Florence Grappin, Philippe Delaye, Y. Arakawa, K. Kuroda, Gérald Roosen

Simultaneous determination of the index and absorption gratings in multiple quantum well photorefractive devices designed for laser ultrasonic sensor

T. Shimura [a,b], F. Grappin [a], P. Delaye [a], S. Iwamoto [b], Y. Arakawa [b], K. Kuroda [b], and G. Roosen [a]

[a] *Laboratoire Charles Fabry de l'Institut d'Optique, Bat 503, Centre Scientifique 91403 Orsay cedex, France*

[b] *Institute of Industrial Science, University of Tokyo, 4-6-1 Komaba, Meguro-ku, Tokyo 153-8505 Japan*

abstract

A new method to determine complex amplitudes of index and absorption gratings in photorefractive multiple quantum wells is presented. In usual method to evaluate these parameters, spectral measurement of absorption change due to the applied field over a wide wavelength range is required and the index change is calculated through the Kramers-Krönig's relationship. In our method, only a set of measured data for photorefractive two-wave mixing set-up with small sinusoidal phase modulation for fixed wavelength is needed. This is thus well adapted to insitu characterization of systems that operate at a given wavelength. Real and imaginary part of the gains owing to the index and the absorption gratings are calculated from the output signals of the system. We apply this method to our photorefractive multiple quantum devices operating at 1064 nm, and obtain consistent results.

Laser ultrasonic sensor with photorefractive two-wave mixing is quite useful because of its high sensitivity and adaptive nature.[1-6] Slow noise component compared to the response time of the photorefractive material is compensated, and wave-front matching is automatically maintained with real time recording of the interference fringe. High sensitivity is also one of the advantages of this method. Sub-nanometer vibration of the scattering surface is easily detected by this system with small power CW-lasers.

Within various photorefractive materials, bulk semiconductors such as CdTe:V and InP:Fe have shown quite good performance for these systems, and the sensitivity of the systems with these materials is close to interferometric limit[4,5]. Photorefractive multiple quantum wells (PR-MQWs) have also been proved that they have good properties for this purpose, especially a higher cut off frequency for compensating the turbulences due to their faster response speed[6,7]. Recently, InGaAs/GaAs PR-MQWs sensitive at 1064 nm have been developed[8] and applied to the vibration detection system[9]. The advantage of this material is, of course, that compact, high power, and high coherence Nd:YAG laser is usable as a laser source.

It is rather easy to consider the optimum operating condition in these systems when the only index grating exists. In this case, photorefractive phase shift ϕ_p, which is the phase shift between the fringe pattern and the space charge field grating, should be 0 or π, and simply larger amplitude of the index grating gives the larger output signal [5]. On the other hand, in PR-MQWs, the situation is more complicated because both index and absorption gratings exist at the same time [7]. To find the optimum operating condition, we need to measure the electro-absorption spectrum over a wide range of wavelength, and calculate index change through the Kramers-Krönig's relationship, then the excitonic spectral phase is obtained from the ratio of the index to absorption variation. The knowledge of this spectral phase allows to choose the operating wavelength that maximizes the devices performances, i.e. the detection sensitivity. In the case of system operating with Nd:YAG lasers the tunability of the laser is not sufficient to see sizeable variation of the spectral phase, and this parameter even if useful for characterization of the structure, brings too much information when regarding device performances.

In this paper, we present a complementary method to determine the amplitude and the phase of both index and absorption gratings, that brings all the required information in a simple manner using the known symmetries of the grating written in the PR-MQW structure. We make a simple two-wave mixing and electro-absorption measurements for positive and negative electric field to determine the amplitudes of the index and absorption gratings simultaneously and photorefractive phase shift without any wavelength scan.

In PR-MQWs, both absorption and index gratings, will contribute to the phase demodulation in the photorefractive laser ultrasonic sensor. Using an usual two wave mixing architecture, we can calculate the optical field for the probe beam at the output of the crystal at time *t*, in case of the high pump to signal intensity ratio :

$$E_s(t) = E_s(0)e^{-\alpha L/2}\left[e^{i\varphi(t)} + \left(e^{(\gamma_n+\gamma_\alpha)L} - 1\right)\right], \qquad (1)$$

where γ_n and γ_α are the photorefractive gain due to the index and absorption gratings respectively, α is the absorption of the material, $\varphi(t)$ is the phase modulation carried by the probe beam, and *L* is the length of the crystal. The photorefractive gains $\gamma_{n,\alpha}$, is related to the amplitude of the index and the absorption gratings Δn and $\Delta\alpha$ as :

$$\gamma_n = -i\frac{2\pi\Delta n}{\lambda} \quad \text{and} \quad \gamma_\alpha = \frac{\Delta\alpha}{2}. \qquad (2)$$

In the index grating definition, the *-i* term deals with the $-\pi/2$ phase shift acquired by the diffracted beam due to the diffraction on a phase grating. It adds to the phase shift between the space charge field grating and illumination pattern ϕ_p, which equals to $\pi/2$ when only the diffusion contributes to the carrier migration. We can then define a new phase shift $\phi_0=\phi_p-\pi/2$. For the absorption grating, this additional phase shift does not exist and the phase shift is only due to the nature of the absorption grating. In the case of PR-MQW the absorption grating is an electro-absorption grating that is in phase with space charge field grating and the phase shift is equal to ϕ_p ($=\phi_0+\pi/2$). This point differs from the case of bulk photorefractive materials in which the absorption grating is due to a population grating in the deep traps

and that is $\pi/2$ phase shifted with the space charge field grating. The electro-absorption nature of the gratings (both index and absorption) has another consequence linked to the quadratic nature of the electro-absorption phenomenon. The index and the absorption grating are proportional to the applied field and the space charge field : $E \cdot E_{sc}$. Thus the photorefractive gains $\gamma_{n,\alpha}$, which are complex quantities, write as :

$$\gamma_n = \gamma_n' + i\gamma_n'' = (E/|E|)|\gamma_n| e^{i\phi_0}, \quad (3)$$

and

$$\gamma_\alpha = \gamma_\alpha' + i\gamma_\alpha'' = (E/|E|)|\gamma_\alpha| e^{i(\phi_0+\pi/2)}. \quad (4)$$

Knowing the symmetry of the phase shift ϕ_0, we can deduce the symmetries of the gain regarding the sign of the applied field. The applied field induces a displacement of the space charge field from its $\pi/2$ phase shifted position at zero field, in a direction that depends on the sign of the electric field. That leads to the symmetry relation : $\phi_0(-E)=-\phi_0(E)$, from which we deduce :

$$\begin{cases} \gamma_n'(-E) = -\gamma_n'(E) = -(E/|E|)|\gamma_n|\cos\phi_0 \\ \gamma_n''(-E) = \gamma_n''(E) = (E/|E|)|\gamma_n|\sin\phi_0 \end{cases}, \quad (5)$$

and,

$$\begin{cases} \gamma_\alpha'(-E) = \gamma_\alpha'(E) = -(E/|E|)|\gamma_\alpha|\sin\phi_0 \\ \gamma_\alpha''(-E) = -\gamma_\alpha''(E) = -(E/|E|)|\gamma_\alpha|\cos\phi_0 \end{cases}. \quad (6)$$

These symmetry relations will be the main point that will allow the independent extraction of the real and imaginary parts of the gains from the experimental data.

From Eq. (1), we calculate the intensity at the output of the crystal with the assumption of the small phase modulation ($\varphi(t)<<\pi/2$) [10] :

$$I_s(t) = I_{s0} e^{-\alpha x}\left\{e^{2(\gamma_n'+\gamma_\alpha')L} - 2e^{(\gamma_n'+\gamma_\alpha')L}\sin[(\gamma_n''+\gamma_\alpha'')L]\varphi(t)\right\}. \quad (7)$$

This is a classical relation in which we simply add the absorption grating term. The gains $\gamma_{n,\alpha}$ depends on the applied electric field, as well as the absorption α of the structure, that has to be independently determined.

Experimentally, we applied on the probe beam a known sinusoidal phase modulation $\varphi(t) = \sqrt{2}\varphi_{RMS}\sin(\omega t)$, and measure its transformation into an intensity modulation through the written grating. The detected signal is thus given by (using (7)) :

$$I_s(t) = I_M(E) + \sqrt{2} I_{RMS}(E)\sin(\omega t), \quad (8)$$

where we also consider the energy transfer from the pump beam to the probe beam, that causes a change in the mean intensity $I_M(E)$ of the probe beam. The mean probe intensity also changes due to the electroabsorption, that is determined with the same experimental setup by a simple measurement of the mean probe intensity with cross polarized beams (i.e. without grating):

$$I_\perp(E) = I_{s0} e^{-\alpha(E)L}. \quad (9)$$

Comparing the Eq. (7) and (8), we obtain, using relation (9) :

$$I_M(E) = I_\perp(E) e^{2(\gamma'(E)+\gamma_\alpha'(E))L}, \quad (10)$$

$$I_{RMS}(E) = -2\varphi_{RMS}\sqrt{I_\perp(E) I_M(E)}\sin[(\gamma_n''(E)+\gamma_\alpha''(E))L]. \quad (11)$$

Now using the symmetry relation of the gains, we can easily show that a measurement of these three quantities $(I_\perp(E), I_M(E), I_{RMS}(E))$ with equal positive and negative values of the applied electric field allows to determine :

$$\begin{cases} [\gamma_n'(E)+\gamma_\alpha'(E)]L = \frac{1}{2}\mathrm{Log}\left(\frac{I_M(E)}{I_\perp(E)}\right) \\ [-\gamma_n'(E)+\gamma_\alpha'(E)]L = \frac{1}{2}\mathrm{Log}\left(\frac{I_M(-E)}{I_\perp(-E)}\right) \end{cases} \quad (12)$$

and

$$\begin{cases} [\gamma_n''(E)+\gamma_\alpha''(E)]L = -\arcsin\left(\dfrac{I_{RMS}(E)}{2\varphi_{RMS}\sqrt{I_\perp(E)I_M(E)}}\right) \\ [\gamma_n''(E)-\gamma_\alpha''(E)]L = -\arcsin\left(\dfrac{I_{RMS}(-E)}{2\varphi_{RMS}\sqrt{I_\perp(-E)I_M(-E)}}\right) \end{cases} \quad (13)$$

from which the real and imaginary part of the two gains are easily calculated.

We evaluated the real and imaginary components of index and absorption gratings with the ultrasonic detection measurement and the method above. The samples were two InGaAs/GaAs PR-MQWs devices. These two samples named sample 1 and 2 have the same structure and made through same procedure as described in ref [8]. They have 100 periods of $In_{0.25}Ga_{0.75}As$ wells and GaAs barriers whose thicknesses are 10 nm and 5 nm respectively. After the sample growth by metal-organic chemical-vapor deposition, 3 MeV protons are irradiated to make samples semi-insulating. Au-Ge alloy electrodes, whose separation is 1 mm, are deposited upon the MQWs. The samples operating in the Franz-Keldysh geometry [11], in which the external field is parallel to the MQW layers.

Experimental setup was based on two-wave mixing configuration. Probe beam was s-polarized. Pump beam was s-polarized for the measurement of $I_M(E)$ and $I_{RMS}(E)$ in Eq. (8), and was p-polarized to measure $I_\perp(E)$ defined in Eq. (9). Pump beam covered the entire region of gap of the two electrodes, which is 1 mm, and the intensity was 20 mW/cm^2. Probe beam was issued from a scattering target imaged just in front of the sample giving a spot radius on the sample of 0.5 mm. The pump probe intensity ratio was 100 approximately. Grating spacing was 3 μm, which is slightly larger than the cut off grating period[8]. We applied the external field for 50 ms every 1 second.

The measured values for $I_M(E)$, $I_\perp(E)$ normalized to the probe intensity I_{s0} when no external field was applied are shown in Fig. 1. The normalized output intensity without grating, $I_\perp(E)$ has the expected quadratic shape due to the change of the electro-absorption proportional to the square of the electric field. Electro-absorption was decreased when the field is applied and the amount of the change was almost the same for both samples. The mean intensity with grating $I_M(E)$ contains the effect of electro-absorption and energy transfer due to the two-wave mixing (and to real part of the index and the absorption gains). The behaviour of the two tested sample is very different. The sign of the energy transfer changed with the change of the direction of the field in sample 1, whereas the sign does not change in sample 2. This result implies that the index grating (real part is an odd function of the field) is dominant for sample 1 and that the absorption grating (even function) is dominant for sample 2.

Root mean square (RMS) values of the AC part of the output probe beams I_{RMS} for the samples 1 and 2 are shown in Fig. 2. The amplitudes of the phase modulation in RMS, φ_{RMS} were 67.9 and 282 mrad for the measurement of sample 1 and 2 respectively. Sample 2 requires larger phase modulation in order to have enough signal for the measurement due to its relatively low sensitivity. Signs of the output signal were opposite for the reversed field for sample 2, on the contrary to the sample 1. Output signal was very small when the applied field was near 10 kV for sample 1 and from zero to -5 kV for the sample 2. It corresponds to the field where $\gamma_n''(E)+\gamma_\alpha''(E)=0$. The output signal contains small 2ω component in these points, especially in the case of the measurement of sample 2 because of large phase modulation. Only ω component was extracted by Fourier analysis of the signal for the data shown in Fig.2. Also, the noise component of each data point is compensated, under the assumption that the RMS value of the output for E=0 comes from the noise component only.

Real and imaginary parts of the index and absorption gratings are calculated from these data by Eqs. (12) and (13). Both index and absorption gratings existed in sample 1 and almost only absorption grating were seen in sample 2, especially the contribution of the index grating to the phase detection is quite small because $\gamma_n''L$ is almost zero. From the results of $I_\perp(E)$ shown is Fig. 1, the sign and the magnitude of absorption change is the same for both samples, and these results are consistent with the results shown in Fig. 3, which show similar values of the absorption gain in both samples. Imaginary parts of the index and absorption gratings have same amplitude and opposite sign for sample 1 as shown in Fig 3(a), these two gratings works cooperatively under the negative field and destructively for the positive field. These results well agree with the results shown in Fig.2(a), in which the sensitivity

becomes small for the positive field.

From the experimental data we can also estimate the phase shift ϕ_0, using equations (5) and (6). For an applied electric field around 10kV.cm^{-1}, we deduce for sample 1 a phase shift $\phi_0=-0.8\pi\pm0.1\pi$ for both index and absorption gratings. In the same condition we calculate for sample 2, $\phi_0=-0.8\pi\pm0.1\pi$ for the absorption grating and $\phi_0=0$ for the index grating. The π difference in the value of the phase shift for the index grating in the two samples corresponds to a change of the sign of the index grating variation with the applied electric field. The origin of this difference is mainly due to a shift of the excitonic absorption peak compared to the fixed used wavelength. We operate close to a minimum value of the index change and the slight change of the exciton wavelength is sufficient to cross the zero level of the index change with wavelength. This corresponds to a value of the excitonic spectral phase, as defined by Nolte et al. [7], close to zero and that changes its sign between the two samples.

In the two samples, the phase shift of the space charge field grating ϕ_P, is the same and is close to $\pi/2$. This parameter linked to the carrier migration mechanism in PR-MQW, is expected to be identical for every sample, if we suppose that they have similar value of the trap density.

In conclusion, we have introduced a new method to evaluate the photorefractive properties of PR-MQWs at fixed wavelength which is used in the laser ultrasonic detection system. The phase and amplitude of the index and absorption gratings is determined from a pair of experimental data for positive and negative applied field without the usage of any spectroscopic measurement. Experimental results were all consistent each other and showed good agreement with the photorefractive properties in PR-MQWs.

references

[1] R. K. Ing and J.-P. Monchalin, Appl. Phys. Lett., 59 (1991) 3233.
[2] A. Blouin and J.-P Monchalin, Appl. Phys. Lett., 65 (1994) 932.
[3] T. Honda, T. Yamashita, and H. Matsumoto, Jpn. J. Appl. Phys., 34, (1995) 3737.
[4] L.-A. de Montmorillon, P. Delaye, J. C. Launay, and G. Roosen, J. Appl. Phys. 82 (1997) 5913.
[5] P. Delaye, A. Blouin, D. Drolet, L.-A. de Montmorillon, G. Roosen, and J.-P. Monchalin, J. Opt. Soc. Am. B, 14 (1997) 1723.
[6] I. Lahiri, L. J. Pyrak-Nolte, D. D. Nolte, M. R. Kruger, G. D. Bacher, and M. B. Klein, Appl. Phys. Lett., 73 (1998) 1041.
[7] D. D. Nolte, T. Cubel, L. J. Pyrak-Nolte, and M. R. Melloch, J. Appl. Opt. Am. B, 18 (2001) 195.
[8] S. Iwamoto, S. Taketomi, H. Kageshima, M. Nishioka, T. Someya, Y. Arakawa, K. Fukutani, T. Shimura, K. Kuroda,, Opt. Lett., 26 (2001) 22.
[9] T. Shimura, S. Iwamoto, H. Kageshima, S. Taketomi, M. Nishioka, T. Someya, Y. Arakawa, K. Fukutani, K. Kuroda, Opt. Mater. 18 (2001) 183.
[10] P. Delaye, L.-A. de Montmorillon, and G. Roosen, Opt. Commun., 118 (1995) 154.
[11] D. D. Nolte and M. R. Melloch, in *Photorefractive Effects and Materials*, D. D. Nolte, ed. (Kluwer, Dordrecht, The Netherlands, 1995), Chap. 7.

Figure captions

Fig. 1. Measured values for the output probe intensities normalized to the value without external field for (a) sample 1, and (b) sample 2. Open rectangles give the output without photorefractive two-wave mixing by cross polarized pump and probe: ($I_{\perp}(E)$). Solid circle gives the output probe intensity with energy transfer through photorefractive two-wave mixing: ($I_M(E)$).

Fig. 2. Experimental results of the detected signals $I_{RMS}(E)$, i.e. rms value of the ac component of the output probe intensity, for (a) sample 1, and (b) sample 2. Values are normalized to the output probe intensity with no applied field.

Fig.3. Calculated photorefractive gains from the experimental data shown in Figs. 1 and 2, for (a) the sample 1, and (b) the sample 2. Solid rectangles and circles give real and imaginary parts of index gratings γ_n'L and γ_n"L. Open rectangles and circles give real and imaginary parts of the absorption, γ_α'L and γ_α"L.

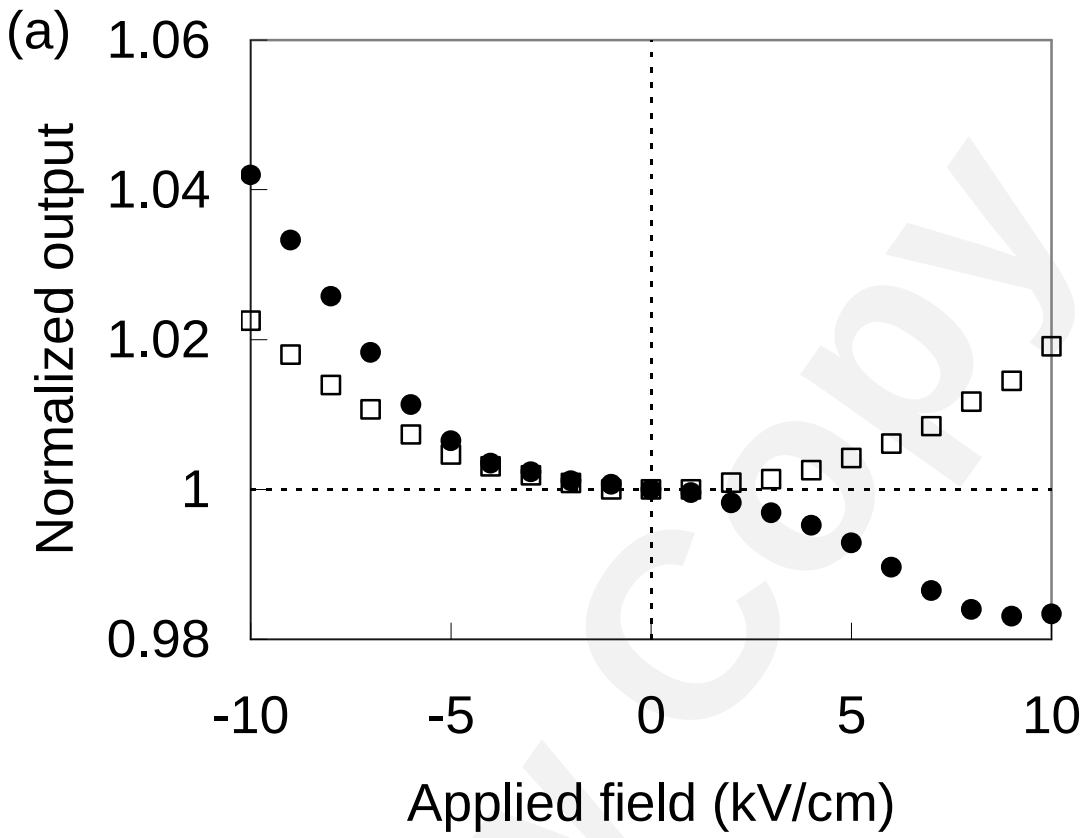

50 %

Fig.1 (a)

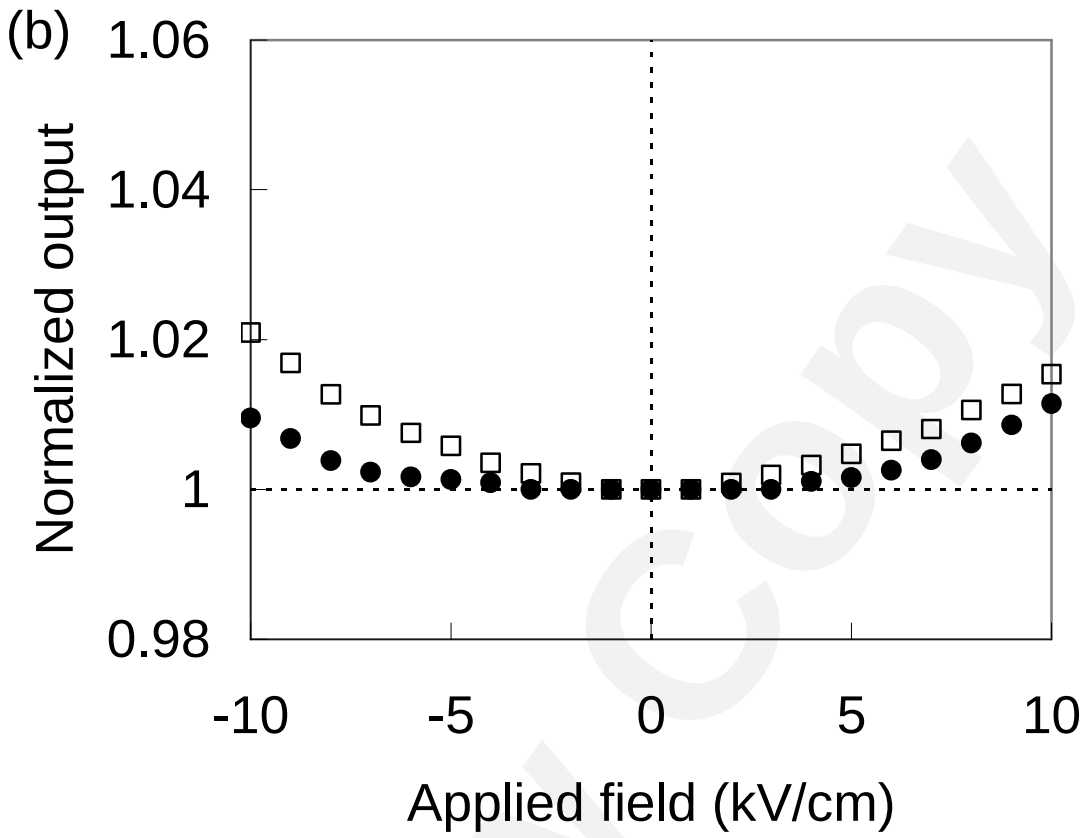

50 %

Fig.1 (b)

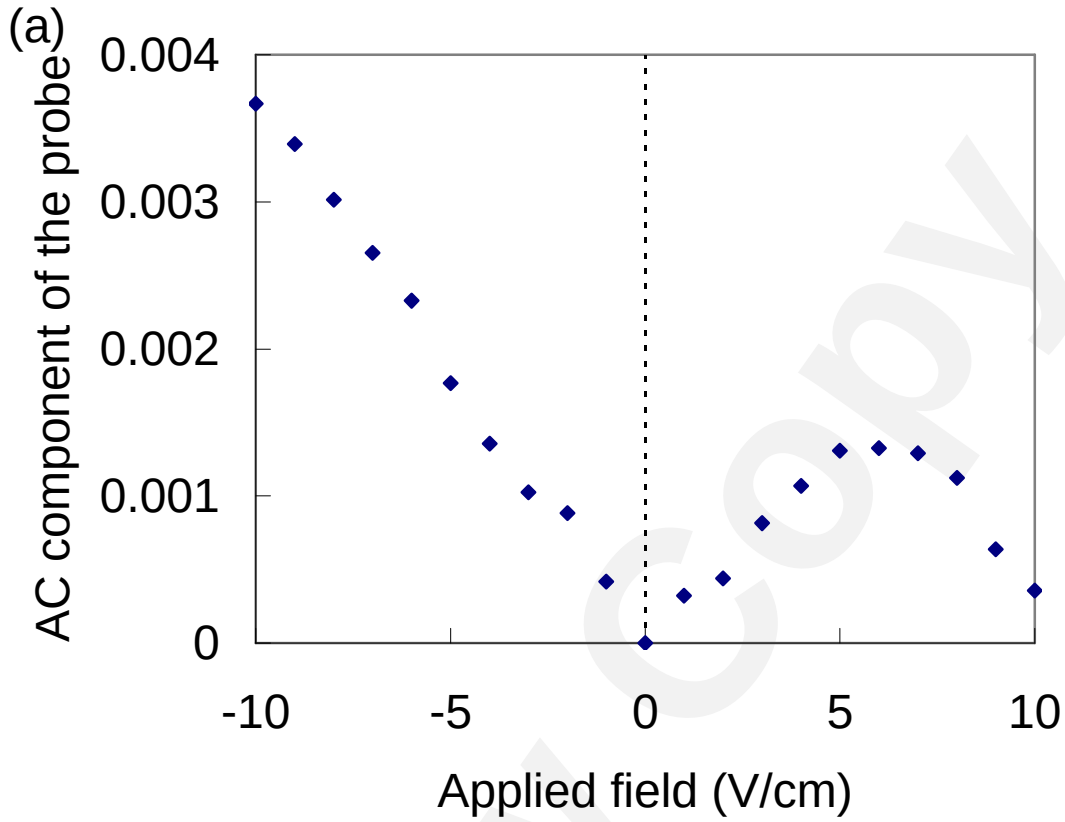

50 %

Fig.2 (a)

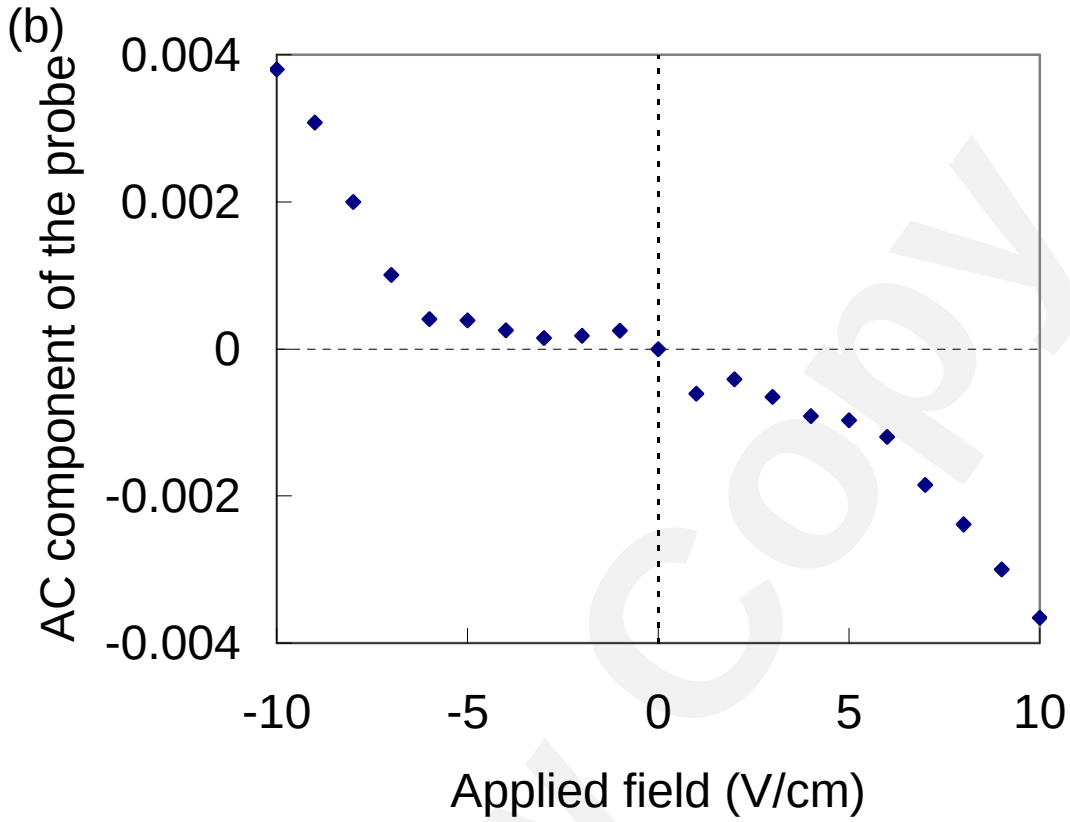

50 %

Fig.2 (b)

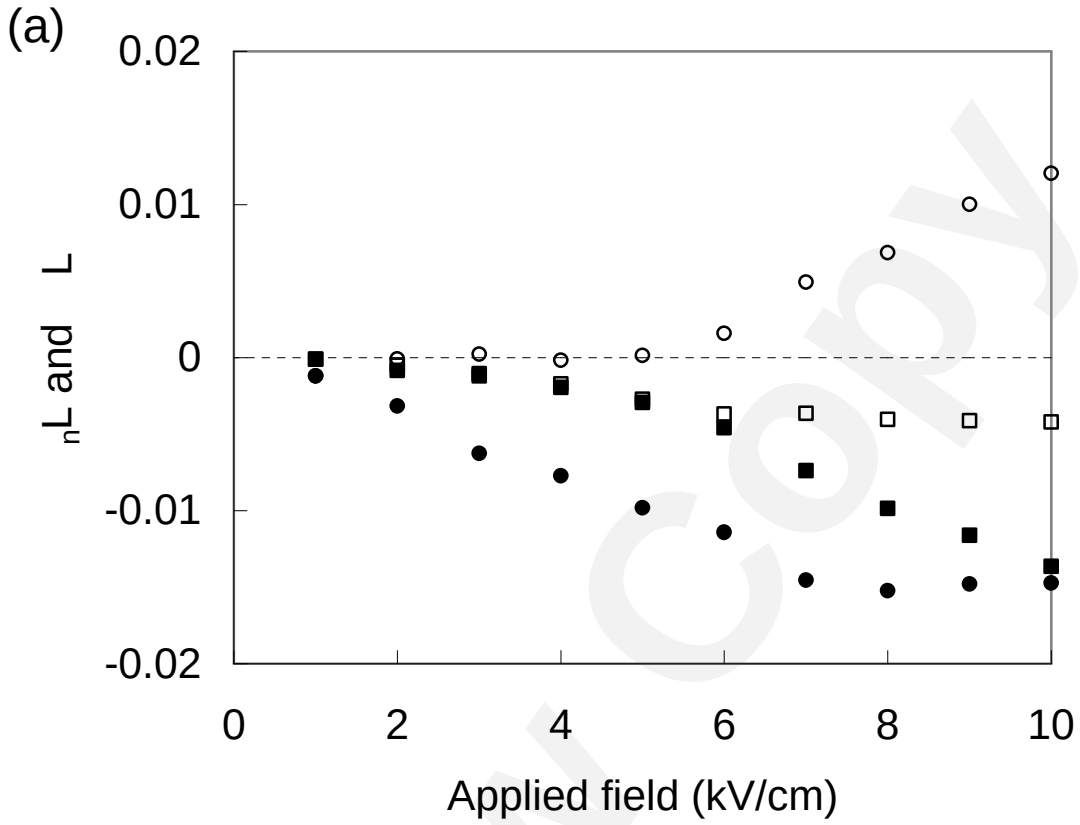

50 %

Fig.3 (a)

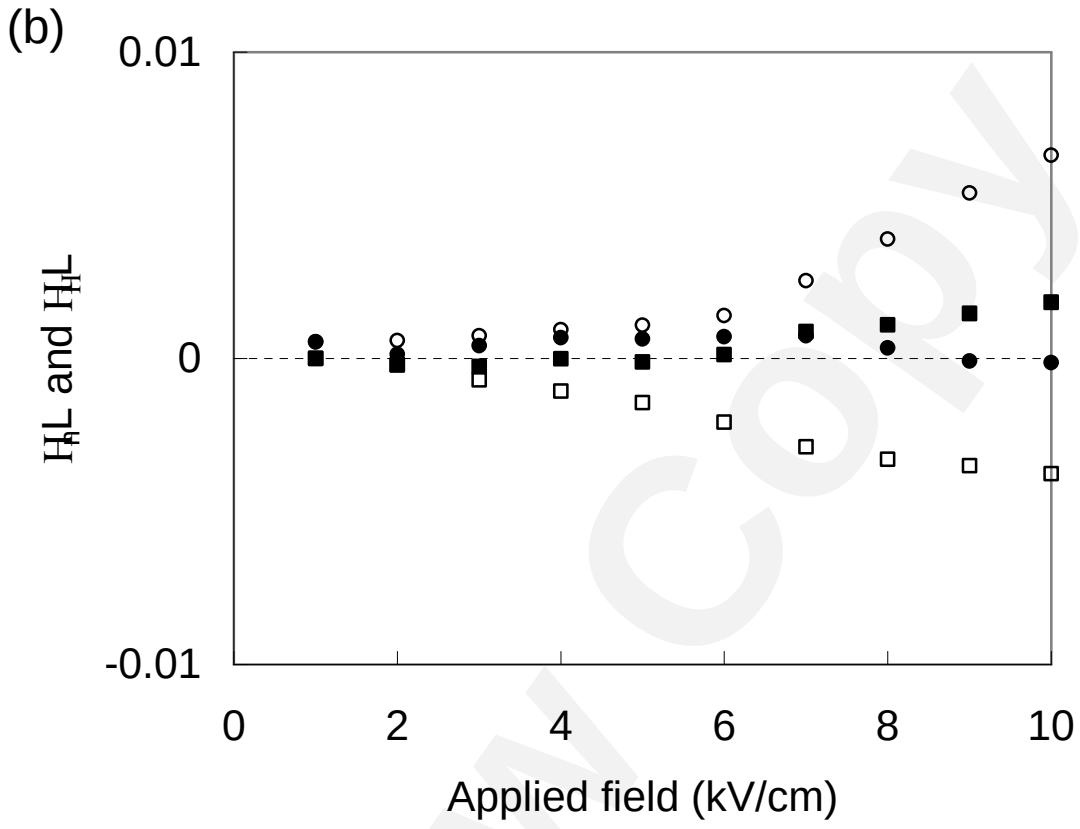

50 %

Fig.3 (b)